Simulation of wave-function microscopy images of Stark resonances

L. B. Zhao, D. H. Xiao, and I. I. Fabrikant

Phys. Rev. A **91**, 043405 — Published 10 April 2015

DOI: 10.1103/PhysRevA.91.043405

Simulation of wave function microscopy images on Stark resonances

L. B. Zhao[1],* D. H. Xiao[2],† and I. I. Fabrikant[3],‡

[1]*Key Laboratory for Photonic and Electronic Bandgap Materials, Ministry of Education, and School of Physics and Electronic Engineering, Harbin Normal University, Harbin 150025, China*

[2]*College of Physical Sciences and Technology, Heilongjiang University, Harbin 150080, China and*

[3]*Department of Physics and Astronomy, University of Nebraska, Lincoln, Nebraska 68588-0299, USA*

Abstract

Wave function microscopy images for Stark resonance states of H atoms are simulated using the quantum-mechanical formalism developed previously. Spatial distributions of ejected electron current densities are compared with experiment, and a good agreement is shown. The nonzero values of minima in the experimentally observed electron current distributions are reproduced by convoluting the theoretical current distribution with an instrumental function representing uncertainties in the position. Our relative strengths of the ejected electron current densities differ from those calculated with the wave packet propagation technique. We show that for the full convergence of the calculation, the distance between the ionized atom and the detector should exceed 10 μm.

PACS numbers: 32.80.Fb, 07.81.+a, 32.60.+i

*libo.zhao@hrbnu.edu.cn

†xiaodehang@hlju.edu.cn

‡ifabrikant@unl.edu

I. INTRODUCTION

Since it was shown that photoionization of atoms in the presence of static electric fields leads to a spatial interference [1] and that the corresponding wave function can be observed on a macroscopic scale [2], a great deal of theoretical and experimental progress has been made on the wave function microscopy. Ejected photoelectron current densities, produced in photoionization of neutral atoms and photodetachment of negative ions in electric fields can be calculated within the framework of semiclassical theory [1–3]. The first experimental implementation of photodetachment microscopy was accomplished by Blondel *et al.* [4]. The photoelectron currents in detachment of negative ions Br^- were recorded on a position-sensitive detector placed in the plane perpendicular to the applied electric field. The subsequent photoionization microscopy experiment for neutral atoms Xe was performed by Nicole *et al.* [5], and a detailed semiclassical analysis of the Xe experimental results was presented [6].

The semiclassical analysis used in Ref. [6] is incomplete, because it does not incorporate Maslov indices, does not treat tunneling through classically forbidden regions, and does not correct singularities that arise in semiclassical approximations. A semiclassical open-orbit theory (OOT) [7], which incorporates all the effects mentioned above, was presented to describe the dynamics of electron wave propagation in the combined Coulomb and electric fields. The OOT, based on an assumption that the electron wave propagates along classical trajectories, provides a clear and intuitive physical picture for interpretation of structures of observed geometrical interference patterns in photoionization. The reliability of the OOT was confirmed by a fully quantum-mechanical formalism for H atoms in a Stark field [8].

The role of Stark resonances in the interference patterns was studied in the photoionization microscopy experiment [9]. A number of Stark resonances were discerned for Xe atoms. However, many observed resonances were not assigned because of the limitation of semiclassical theory for Stark H atoms used in that paper. Obviously, it is necessary to develop theoretical methods for multielectronic atoms in an external electric field. The pioneering theoretical work in photoionization microscopy for multielectronic atoms was performed by Robicheaux and Shaw [10], based on Harmin's semiclassical theory [11]. Their approach has been applied to explanation of the experiment for Stark Xe atoms [12], and an extensive theoretical investigation for Xe was also reported by Texier [13]. Zhao *et al* [14] developed a

fully quantum-mechanical coupled-channel theory to simulate spatial distributions of electron current densities produced in photoionization for nonhydrogenic atoms in an electric field.

A recent experimental development of photoionization microscopy makes it possible to visualize electron standing waves tunneling through a potential barrier formed by the superposition of the atomic Coulomb field and the uniform external field. The first observations of resonance tunneling have been implemented for Li atoms by Cohen *et al.* [15] and for H atoms by Stodolna *et al.* [16]. The wave function images recorded on a two-dimensional detector clearly display signatures of quasibound electronic states. Their experimental results confirm the theoretical prediction of resonance tunneling made by Zhao and Delos [7, 8]. However, the quasibound resonance states observed in the experiment for H and Li atoms were found to be only in qualitative agreement with those calculated using the wave packet propagation technique. In particular, the nonzero values of the current density at minima observed in the experiment were not reproduced either for H or for Li atoms. The existing discrepancies between experiment and theory stimulated us to perform investigations of wave function microscopy on Stark resonances. The results of these studies for H atoms are presented in the present paper.

II. THEORETICAL OUTLINE

The quantum-mechanical formalism used in this study has been presented in Ref. [8], where theoretical derivation for the outgoing electron wave function and details of numerical integrations of the Schrödinger equations can be found. Here we give only key outlines and list the main formulas related to calculations of electron current densities.

The formalism was developed to simulate spatial distributions of electron current densities, generated in photoionization of H atoms in an external electric field. In the mixed parabolic and semiparabolic coordinates $\xi = \sqrt{r+z}$, $\eta = r - z$, and $\phi = tan^{-1}(y/x)$, we solve the homogeneous Schrödinger equations for bound and continuum states, while the outgoing electron wave functions, incorporating the atom-radiation field interaction, is given by the solution of the inhomogeneous Schrödinger equation which is constructed in terms of the solutions of the homogeneous Schrödinger equations. The outgoing-wave solution is

written as [8]

$$\Psi_{out}(\mathbf{r}) = \int G^{+}(\mathbf{r},\mathbf{r}')D\Psi_{ini}(\mathbf{r}')d\mathbf{r}', \tag{1}$$

where D denotes the dipole operator, $\Psi_{ini}(\mathbf{r}')$ represents the wave function for the initial bound state of the atomic system, and $G^{+}(\mathbf{r},\mathbf{r}')$ is the Green's function satisfying the outgoing-wave boundary condition, given by

$$G^{+}(\mathbf{r},\mathbf{r}') = -i\frac{\pi}{2}\sum_{\beta m}\left[\psi_{\epsilon\beta m}(\mathbf{r}')\right]^{*}\Xi_{\beta}(\xi)\frac{v_{\beta}^{+}(\eta)}{\sqrt{\eta}}\Phi_{m}(\phi), \tag{2}$$

where $\Xi_{\beta}(\xi)$ and $\Phi_{m}(\phi)$ represent the wave function of Stark H atoms in the ξ and ϕ coordinate, $v_{\beta}^{+}(\eta)$ denotes the outgoing wave function in the η coordinate, and $\psi_{\epsilon\beta m}(\mathbf{r}')$ is the three-dimensional orthonormalized wave function,

$$\psi_{\epsilon\beta m}(\xi',\eta',\phi) = \Xi_{\beta}(\xi')\frac{v_{\beta}^{reg}(\eta')}{\sqrt{\eta}}\Phi_{m}(\phi'), \tag{3}$$

where $v_{\beta}^{reg}(\eta')$ is the regular solution of the Schrödinger equations in the η coordinate. The dimensionless ratio of the electron current density to the photon current density in cylindrical coordinates (ρ, z, ϕ) is given by [17]

$$R(\rho, z_{det}, \phi) = \frac{2\pi\omega}{c}\mathrm{Im}\left[\Psi_{out}^{*}(\mathbf{r})\frac{d\Psi_{out}(\mathbf{r})}{dz}\right]_{z=z_{det}}, \tag{4}$$

where ω is the photon frequency, c is the speed of light, and the z_{det} represents the distance from the origin to the detector. This is in fact the differential cross section, but per unit area, rather than per unit solid angle. This ratio can be integrated over the azimuthal angle ϕ, and it is convenient to represent the result as a differential cross section per unit length in the ρ variable

$$\frac{d\sigma\left(\rho, z_{det}\right)}{d\rho} = \int_{0}^{2\pi} R(\rho, z_{det}, \phi)\rho d\phi. \tag{5}$$

In case this does not cause a confusion, $\mathcal{R} = \rho R$ will also be called the electron current density.

III. RESULTS AND DISCUSSION

According to the experimental conditions of Ref. [16], the present calculations assume that ground-state H atoms in an electric field with strength 808 V/cm are resonantly excited to a mixture state of $2s$ and $2p$ by a two-photon transition, and then ionized into states near

ionization threshold by tunable laser pulses. The polarization of the laser is along the applied electric field. Such a polarization leads to the $m = 0$ final ionization states.

Spatial distributions of ejected electron currents were simulated for photoionization into resonance states of H atoms in a Stark field from the initial state $\Psi_{ini}(\boldsymbol{r}) = c_1\psi_{2p_{1/2}}(\boldsymbol{r}) + c_2\psi_{2s_{1/2}}(\boldsymbol{r})$, where $\psi_{2p_{1/2}}(\boldsymbol{r})$ and $\psi_{2s_{1/2}}(\boldsymbol{r})$ denote wave functions for field-free H atoms in the jj representation, and c_1 and c_2 are field-dependent mixing coefficients determined from the corresponding secular equation. Generally, the $\psi_{2p_{3/2}}$ state should be added too, but for the relatively weak field considered in the present paper, $\mathscr{F} = 808$ V/cm, the coupling with the $j = 3/2$ state is so weak that it is negligible. Moreover, our calculations show that the spatial distribution of photoelectron currents is insensitive to the mixing coefficient, apparently because of the dominance of one resonance term in the sum of Eq. (2). Therefore changing the initial state in Eq. (1) leads only to the change of the absolute value of the wave function $\Psi_{out}(\mathbf{r})$, but does not change shape of the distribution. The detector is assumed to be located under the source of H atoms at the distance -1000 μm. This distance is large enough to guarantee convergence of the radial distribution shapes of the ejected electron currents.

The photoelectron images for four resonance states $(n_1, n_2, m) = (0, 29, 0)$, $(1, 28, 0)$, $(2, 27, 0)$, and $(3, 26, 0)$, where n_1 and n_2 are the parabolic quantum numbers and m is the magnetic quantum number, are shown in the left panels of Fig. 1. These images clearly show one, two, three and four bright fringes, respectively, corresponding to the zero, one, two, and three nodes of the wave functions of the four resonances states. In the right panels, differential cross sections or radial distributions of ejected electron currents calculated using the quantum mechanical formalism are compared to the experimental results reported by Stodolna *et al.* [16]. The electron currents convolved with a Gaussian function of FWHM 2000 a_0, corresponding to the experimental resolution of the detector [18], are also illustrated in the figure. A good agreement is observed, and in particular the convolved electron currents reproduce the nonzero values at minima observed in the experiment.

The energies of four resonance states $(0, 29, 0)$, $(1, 28, 0)$, $(2, 27, 0)$, and $(3, 26, 0)$ of H atoms in an electric field with strength 808 V/cm, calculated using the quantum mechanical formalism [8], are compared to the experimental results [16] and those from the semiclassical theory based on the Bohr-Sommmerfeld quantization rule [14] in table I. Our quantum-mechanical calculations are in excellent agreement with both experimental and semiclassical

results.

The present ejected electron current densities produced in photoionization into the four Stark resonance states $(0, 29, 0)$, $(1, 28, 0)$, $(2, 27, 0)$, and $(3, 26, 0)$ of H atoms in an electric field 808 V/cm are compared with those from the wave packet propagation technique [16] in Fig. 2. The peak positions are in good agreement for all the four current density profiles. However, the relative strengths of the electron current densities obviously differ. Considering the fact that no complicated electron correlations occur in the Stark H atom system, such a disagreement is unsatisfactory. The wave packet propagation calculations [16] show the stable spatial distribution of ejected electron currents for these resonances starting from z_{det} $= -$ 0.4 μm on, where z_{det} is the distance from the atomic source to the detector. Such a conclusion is different from ours. We investigated the change of spatial electron current distributions with distances z_{det} for a number of Stark states including these four resonance states using the quantum mechanical formalism [8] and semiclassical open-orbit theory [7], and found that these two theories do not produce the convergent spatial distribution of ejected electron currents at $z_{det} = -$ 0.4 μm. Figure 3 displays the change of spatial electron current distributions with distances z_{det} for the Stark resonance state $(3, 26, 0)$ of H atoms in an electric field 808 V/cm. The electron current density distribution for each z_{det} is drawn together with that at $z_{det} = -$ 1000 μm. The results in Fig. 3 illustrates that convergence of the electron current distributions is reached only beyond $z_{det} = -$ 10 μm.

To explain this result, we can assume that an established current density distribution can occur only at distances significantly exceeding the classical turning point. Thus one may employ the potential barrier, determined by the electric field strength, the parabolic quantum number, and the magnetic quantum number for the final state, to estimate how far the current density distributions may converge away from the atomic source, and therefore it is easy to understand what controls the convergence. For the (2,27,0) resonance, for example, the classical turning point in the η coordinate equals 5404 a.u. This means that the minimum tunnel exit value of z is $-$ 2702 a.u. $= -$ 0.14 μm, and one cannot expect convergent result for the current density distribution if z_{det} is of the same order of magnitude. Our value $z_{det} = -10$ μm is consistent with this estimate.

The pronounced differences between photoelectron images of Stark on-resonance and images of off-resonance states were observed in the experiment [16]. The experiment shows that the signature of the resonance state $(2, 27, 0)$, the two nodes, disappears when the

resonance energy is shifted. We simulated spatial distributions of the electron current densities for the two off-resonance states at $\epsilon = -165.347$ cm^{-1} and -168.257 cm^{-1}. The computed quantum results are compared to experiment in Fig. 4. The complete disappearance of the resonance effect is reproduced for the two off-resonance energies in our calculations, although the electron current distribution for -168.257 cm^{-1} has a peak shift toward $\rho = 0$. We also performed a semiclassical calculation using the open-orbit theory [7]. It is well known that semiclassical waves undergo refraction near a fold-type caustic surface dividing the configuration space into the classically allowed and forbidden regions, and therefore the semiclassical electron wave functions display singularities at the caustic surfaces. The uniform approximation is able to fix such singularities. Here we adopt the uniform approximation developed in Ref. [7] to calculate the electron current densities. The obtained results from the semiclassical and uniform approximations are shown in Fig. 4. The quantum mechanical calculations are in good agreement with the uniform and semiclassical approximations except for the divergence of the semiclassical currents at the caustics.

IV. CONCLUSION

In summary, we have simulated the wave function microscopy images for Stark resonance states of H atoms using the quantum-mechanical formalism. We have compared the calculated spatial distributions of electron current densities with experiment. The results are in good agreement. The nonzero values of minima in the electron current distribution, corresponding to the Stark resonance states experimentally observed, are reproduced by convoluting the theoretical results with the instrumental function. However, our relative strengths of the ejected electron current densities differ from those calculated with the wave packet propagation technique. Our quantal calculations show that the electron current distributions are convergent only beyond 10 μm from the atomic source, but the wave packet propagation technique gives stable electron current distributions beyond 0.4 μm from the atomic source. From the calculation of classical turning points for the electron motion, we conclude that our distance of convergence is more physically reasonable. Furthermore, we simulated spatial distributions of the electron current densities at off-resonance energies using the quantal formalism, the semiclassical and uniform approximation. The complete disappearance of the the resonance effect is observed for the off-resonance energies.

Acknowledgments

We would like to thank Dr. A. S. Stodolna and Professor M. J. J. Vrakking for providing their experimental and theoretical data. This work was supported by the NSF of China under Grant No 11474079 and the NSF of USA under Grant No. PHY-1401788.

---

[1] I. I. Fabrikant, JETP **52**, 1045 (1980).

[2] Yu. N. Demkov, V. D. Kondratovich, and V. N. Ostrovsky, JETP Lett. **34**, 403 (1981).

[3] V. D.Kondratovich andV. N. Ostrovsky, J. Phys. B **17**, 1981 (1984); **17**, 2011 (1984); **23**, 21 (1990); **23**, 3785 (1990).

[4] C. Blondel, C. Delsart, and F. Dulieu, Phys. Rev. Lett. **77**, 3755 (1996).

[5] C. Nicole, H. L. Offerhaus, M. J. J. Vrakking, F. Lépine, and C. Bordas, Phys. Rev. Lett. **88**, 133001 (2002).

[6] C. Bordas, F. Lépine, C. Nicole, and M. J. J. Vrakking, Phys. Rev. A **68**, 012709 (2003).

[7] L. B. Zhao and J. B. Delos, Phys. Rev. A **81**, 053417 (2010).

[8] L. B. Zhao and J. B. Delos, Phys. Rev. A **81**, 053418 (2010).

[9] F. Lépine, C. Bordas, C. Nicole, and M. J. J. Vrakking, Phys. Rev. A **70**, 033417 (2004).

[10] F. Robicheaux and J. Shaw, Phys. Rev. A **56**, 278 (1997).

[11] D. A. Harmin, Phys. Rev. A **24**, 2491 (1981); **26**, 2656 (1982).

[12] C. Nicole, I. Sluimer, F. Rosca-Pruna, M. Warntjes, M. J. J. Vrakking, C. Bordas, F. Texier, and F. Robicheaux, Phys. Rev. Lett. **85**, 4024 (2000).

[13] F. Texier, Phys. Rev. A **71**, 013403 (2005).

[14] L. B. Zhao, I. I. Fabrikant, J. B. Delos, F. Lépine, S. Cohen, and C. Bordas, Phys. Rev. A **85**, 053421 (2012).

[15] S. Cohen, M. M. Harb, A. Ollagnier, F. Robicheaux, M. J. J. Vrakking, T. Barillot, F. Lépine, and C. Bordas, Phys. Rev. Lett. **110**, 183001 (2013).

[16] A. S. Stodolna, A. Rouzeé, F. Lépine, S. Cohen, F. Robicheaux, A. Gijsbertsen, J. H. Jungmann, C. Bordas, and M. J. J. Vrakking, Phys. Rev. Lett. **110**, 213001 (2013).

[17] I. I. Fabrikant, J. Phys. B **23**, 1139 (1990).

[18] A typical experimental resolution of the detector is taken into account to be $50 \sim 100$ μm if

TABLE I: Comparison of resonance positions (in cm^{-1}) for H atoms in an electric field with strength 808 V/cm between the present calculations (FQM: fully quantum-mechanical results; SC: semiclassical results) and experiment (Exp.) [16].

(n_1, n_2, m)	FQM	SC	Exp.
(0,29,0)	-172.809	-172.745	-172.82
(1,28,0)	-169.617	-169.558	-169.67
(2,27,0)	-166.427	-166.377	-166.45
(3,26,0)	-163.240	-163.199	-163.30

the diameter of the images is $1 \sim 3$ mm.

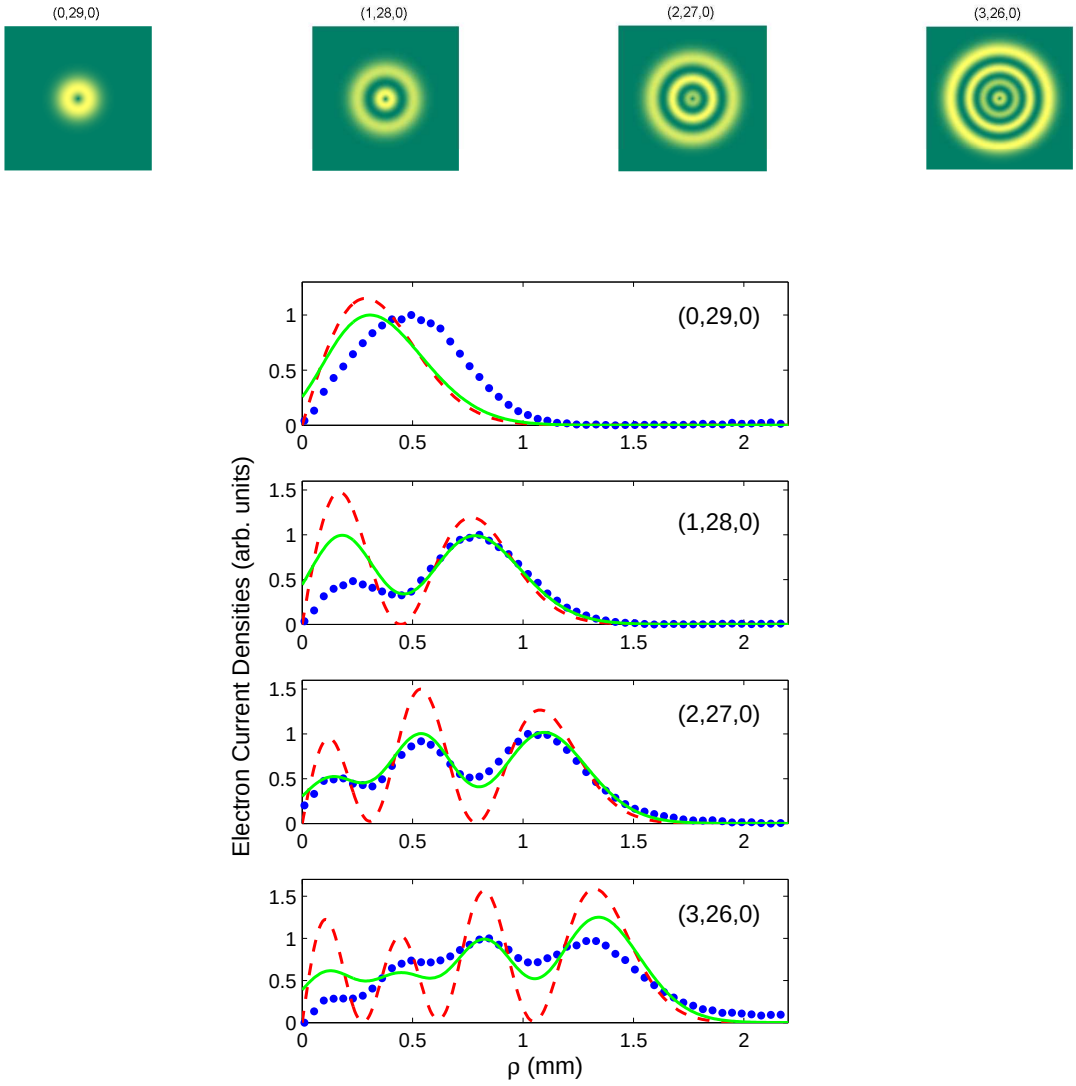

FIG. 1: (To editor: the four photoelectron images should be arranged in one column of the left panel, corresponding to each subfigure in the right panel.) (Color online) Differential cross sections or radial distributions of ejected electron currents in photoionization into four given resonance states $(0, 29, 0)$, $(1, 28, 0)$, $(2, 27, 0)$, and $(3, 26, 0)$ of H atoms from a mixture of $2s$ and $2p$ states at an electric field 808 V/cm. The four resonance states are located at -172.809 cm^{-1}, -169.617 cm^{-1}, -166.427 cm^{-1}, and -187.029 cm^{-1}, respectively. The simulated photoelectron images are shown in the left panels, while the experimental and computational electron currents are compared in the right panels. The blue dots, red dashed curves and solid green curves represent the experimental measurements, the calculated electron current densities and these current densities convolved with the experimental resolution of the detector. Note that for the purpose of comparison, the calculated results in the right panel are scaled to the macroscopic dimensions of the experiment.

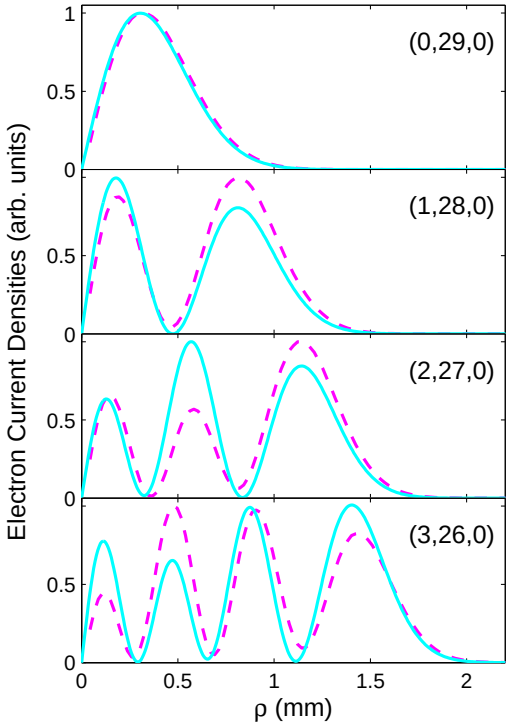

FIG. 2: (Color online) Comparison of the computed electron current densities in photoionization into the resonance state $(0, 29, 0)$, $(1, 28, 0)$, $(2, 27, 0)$, and $(3, 26, 0)$ of H atoms from a mixture state of $2s$ and $2p$ at an electric field 808 V/cm. The cyan solid curves and dashed magenta curves denote the present results and those from the wave packet propagation technique [16].

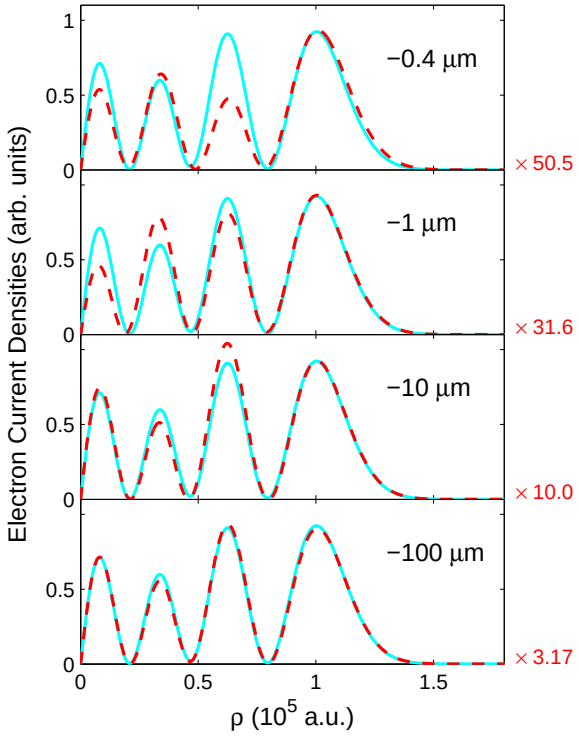

FIG. 3: (Color online) The change of spatial electron current distributions with distances z_{det} of the atomic sources for the resonance state $(3, 26, 0)$ of H atoms in an electric field 808 V/cm. The resonance state is located at $-$ 163.240 cm^{-1}. The cyan solid curves represent the electron current density distributions at $z_{det} = -$ 1000 μm, while the red dashed curves denote those at $z_{det} = -$ 0.4 μm, $-$ 1.0 μm, $-$ 10 μm, and $-$ 100 μm. Note: the electron current distributions spread out with increasing z_{det}, and therefore ρ of the red dash curve in each panel is multiplied by a factor denoted.

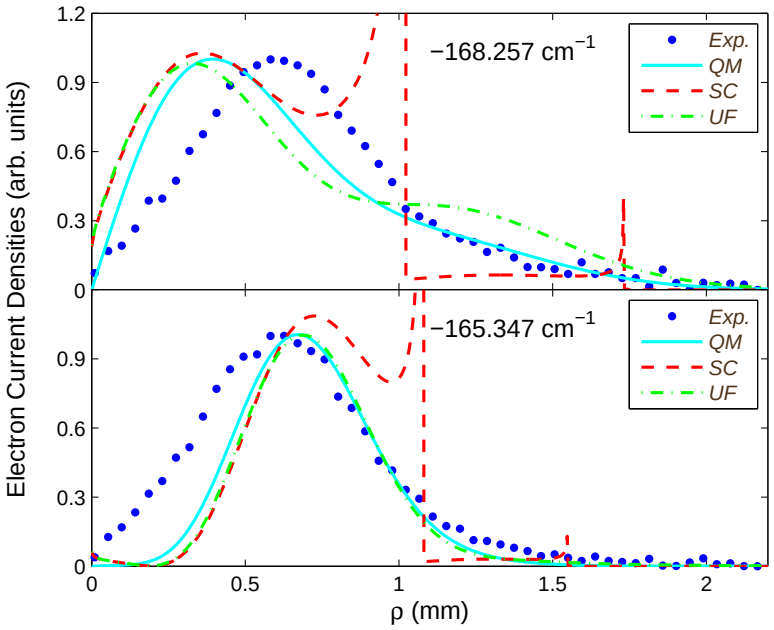

FIG. 4: (Color online). Comparison of electron current distributions for off-resonance states of Stark H atoms in an electric field 808 V/cm. The two off-resonance states are located at $\epsilon = -165.347\ \mathrm{cm}^{-1}$ and $-168.257\ \mathrm{cm}^{-1}$. Experiment: ● Stodolna *et al.* [16] (Exp.). Theory: —— present quantum mechanical calculation (QM); - - - - present semiclassical calculation (SC) using open-orbit theory; - ·- · present calculation using the uniform approximation. Note: the semiclassical electron currents diverge at caustics corresponding to the red dashed vertical lines.